

# ChemComm

Accepted Manuscript



This is an *Accepted Manuscript*, which has been through the Royal Society of Chemistry peer review process and has been accepted for publication.

*Accepted Manuscripts* are published online shortly after acceptance, before technical editing, formatting and proof reading. Using this free service, authors can make their results available to the community, in citable form, before we publish the edited article. We will replace this *Accepted Manuscript* with the edited and formatted *Advance Article* as soon as it is available.

You can find more information about *Accepted Manuscripts* in the [Information for Authors](#).

Please note that technical editing may introduce minor changes to the text and/or graphics, which may alter content. The journal's standard [Terms & Conditions](#) and the [Ethical guidelines](#) still apply. In no event shall the Royal Society of Chemistry be held responsible for any errors or omissions in this *Accepted Manuscript* or any consequences arising from the use of any information it contains.

## COMMUNICATION

# $\beta$ -Tetrachlorotetramethoxyporphycenes: positional effect of substituents on structure and photophysical properties†

Cite this: DOI: 10.1039/x0xx00000x

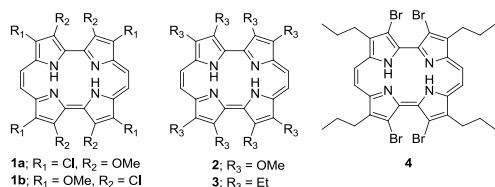
Received 00th January 2012,  
Accepted 00th January 2012Anup Rana<sup>a</sup> and Pradeepta K. Panda<sup>a</sup>

DOI: 10.1039/x0xx00000x

www.rsc.org/

We report the regiospecific synthesis of first chloro substituted porphycenes as two positional isomers of  $\beta$ -tetrachlorotetramethoxyporphycene. The positional effect of the substituents on these isomers could be clearly distinguished in their structure and photophysical properties.

Porphycene reported by Vogel is the first constitutional aromatic isomer of porphyrin.<sup>1a</sup> Its unique intense absorption in red region compared to latter, make it one among the best choices of photosensitizer for photodynamic therapy (PDT).<sup>1</sup> Further, porphycenes have also been explored for their potential application in the field of protein mimicry, catalysis, material chemistry, nonlinear optical studies and most recently for dye sensitized solar cell application.<sup>2</sup> Owing to its rectangular

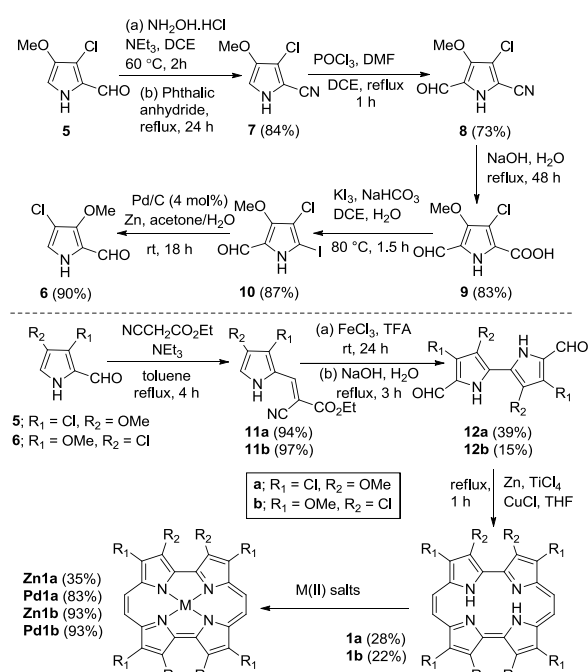


coordination core, porphycene displays strong NH...N hydrogen bonding. Therefore, NH-tautomerism, double hydrogen transfer study and excited state photodynamics of this macrocycle are of great fundamental interest.<sup>3</sup> Recently, we found fusion of  $\beta$ - $\beta'$  bipyrrolic positions of porphycene led to unprecedented square type metallo-complexes, along with very interesting laser intensity dependent multiphoton absorption.<sup>2e</sup> Very recently, Hayashi and coworkers demonstrated formation of unusual cis-tautomer of meso dibenzo-fused porphycene.<sup>4</sup>

In spite of many interesting attributes, the studies on porphycene is quite limited due to difficulty associated with the synthesis of the building blocks e.g. bipyrrrole dialdehydes or

bispyrrolylethane.<sup>1,5</sup> In this regard, recently we found octamethoxyporphycene displayed very good lipophilicity and also hydrophilicity, with its Pd(II)-complex producing singlet oxygen efficiently ( $\phi_A$ : 0.73).<sup>6</sup> On the other hand, very recently we noticed replacement of electron donating methoxy groups with electron withdrawing methylthio moieties led to intense large red shifted absorption with unique coalesced Q-bands displaying strong enhancement in two photon absorption cross-sections.<sup>2f</sup> It is well known that properties of porphycene are sensitive to the type of substituent and their positions. However, to the best of our knowledge, the positional effect of substituents in porphycene chemistry is yet to be investigated. The unexpected synthesis of 3-chloro-4-methoxypyrrole-2-aldehyde **5**,<sup>7</sup> help us to explore the synthesis of two positional isomers of first chloro-substituted porphycenes, namely  $\beta$ -tetrachlorotetramethoxyporphycenes **1a** and **1b** along with their metallo-derivatives, to study the positional effect of substituents in their structure, electrochemical and photophysical properties along with the singlet oxygen generation ability ( $\phi_A$ ).

As **5** could be synthesized in good yield<sup>7</sup> and we found Ullmann coupling of its iodo derivative did not yield the desired bipyrrrole dialdehyde (Scheme S1 in ESI†), therefore we decided to explore alternative oxidative coupling approach and towards this, the aldehyde group has to be protected as it is sensitive to the reaction condition. In order to synthesize the other isomeric porphycene **1b**, 4-chloro-3-methoxypyrrole-2-aldehyde **6** emerged as the desired precursor. Towards this we employed **5** as the starting material (Scheme 1). The aldehyde group of **5** was converted to oxime, followed by dehydration with phthalic anhydride under reflux condition to obtain the desired 3-chloro-4-methoxypyrrole-2-nitrile **7** in 84% overall yield.<sup>8</sup> The Vilsmeier-Haack formylation of **7** afforded the aldehyde **8** in 73% yield, whose structure was further confirmed by single crystal XRD (Fig. S23 in ESI†). Subsequent hydrolysis of **8** with aqueous NaOH under reflux condition led

Scheme 1 Synthesis of  $\beta$ -tetrachlorotetramethoxyporphycenes

to the formation of carboxylic acid **9** in 83% yield. However, our repeated effort towards deprotection of **9** under all standard conditions failed. Therefore, we employed decarboxylative iodination of **9** with  $\text{KI}_3/\text{NaHCO}_3$  to form the iodo-derivative **10** in 87% yield, followed by deiodination using catalytic amount of Pd/C with activated Zn, led to the formation of desired  $\alpha$ -free pyrrole aldehyde **6** in 90% yield, whose structure was further confirmed by XRD analysis (Fig. S23 in ESI<sup>†</sup>).<sup>9</sup>

With both the pyrrolic precursors in hand, we proceed to perform oxidative coupling to synthesize the bipyrole dialdehydes (Scheme 1). Towards this the aldehyde group of **5** and **6** was protected to obtain the corresponding cyanoacrylate pyrroles **11a** and **11b** by Knoevenagel condensation, with ethyl 2-cyanoacetate in 94 and 97% yields, respectively.<sup>10</sup> Scholl oxidation of **11a** and **11b** with  $\text{FeCl}_3$  using TFA as solvent, led to the formation of corresponding bipyroles,<sup>11</sup> and without further characterization, the cyanoacrylate groups were deprotected by refluxing in 3M aqueous NaOH to afford the desired bipyrole dialdehydes **12a** and **12b** in 39 and 15% yields, respectively in two steps. Interestingly, our previously developed oxidative coupling method using PIFA and  $\text{BF}_3 \cdot \text{OEt}_2$  on **11a**, followed by deprotection as mentioned above provided the desired **12a** in comparable yield (34%).<sup>2f</sup> However, synthesis of **12b** under identical condition resulted in failure, indicating probably PIFA is not sufficiently strong to activate  $\alpha$ -position of pyrrole **11b**, due to the presence of deactivating chloro group at the adjacent  $\beta$ -position.<sup>12</sup> Further, the structure of **12a** was confirmed by single crystal XRD technique (Fig. S23 in ESI<sup>†</sup>) and very interestingly, it exists in the unusual *cis* conformation. Finally, McMurry coupling of **12a** and **12b** with Zn/ $\text{TiCl}_4$ / $\text{CuCl}$  under reflux condition provided the desired porphycenes **1a** and **1b** in 28 and 22% yields, respectively. Both the freebase porphycenes were further converted to their corresponding Zn(II) and Pd(II) complexes. All the compounds were well characterized by standard spectroscopic techniques.

The  $^1\text{H}$  NMR spectra of freebase porphycenes **1a** and **1b** display very marginal difference in *meso* proton resonances

occurring at 9.80 and 9.65 ppm, whereas significant upfield shift could be noticed in imino proton resonances for **1b** (0.16 ppm) compared to that of **1a** (0.98 ppm). This may be attributed to the greater nonbonding interactions between four bulky chloro substituents at 3,6- and 13,16- positions in **1b** compared to O's of methoxy substituents in **1a**, decreasing the N-H...N hydrogen bonding in case of the former. This could be further confirmed by comparison of  $^1\text{H}$  NMR spectrum of analogous porphycene **2** imino protons with that of **1a** (0.36 vs 0.98 ppm), where the marginal down field shift in case of latter could be attributed to the four electron withdrawing chloro groups.<sup>6</sup>

The UV-Vis spectrum of **1a** in  $\text{CHCl}_3$  consists of split Soret bands at 376 and 384 nm, along with three Q-type bands at 565, 608 and 647 nm, whereas that of **1b** displays Soret band at 385 nm and Q-type bands at 572, 625 and 664 nm (Fig. 1 and Table S1 in ESI<sup>†</sup>). The lowest energy band is 11 and 28 nm red shifted, respectively for **1a** and **1b** compared to octamethoxy analogue **2**,<sup>6</sup> indicating electron deficient nature of these porphycenes. Further, between them, while there is hardly any change in the absorption of the Soret band, the lowest energy band for **1b** is 17 nm red shifted compare to **1a** and this may be

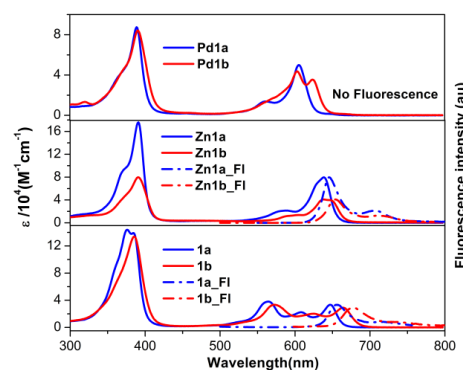
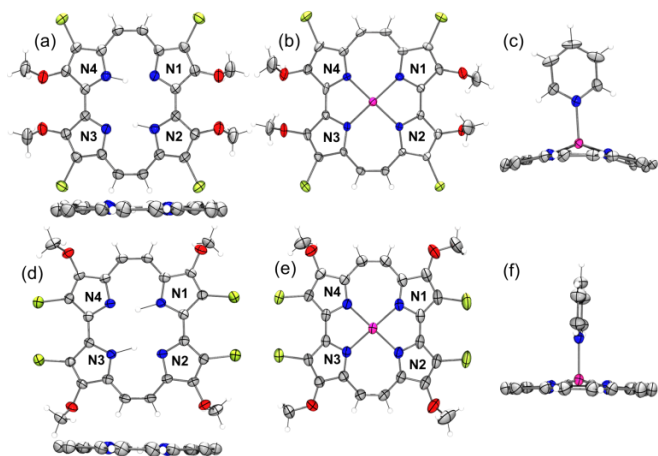


Fig. 1 UV-Vis (solid line) and fluorescence (dot dash line) spectra of **1a** and **1b** along with their Zn(II) and Pd(II) complexes in  $\text{CHCl}_3$  at 25 °C.

attributed to the greater non-bonding interaction between relatively bulky chloro groups at 3,6- and 13,16- positions. This clearly reflects the positional effect of substituents in the two porphycene isomers, which is more evident in their Q-bands than Soret bands, as substituents are expected to perturb only the frontier orbitals significantly. Further, Zn(II) and Pd(II) complexes of **1a** and **1b** consist of red shifted Soret band at 389-391 nm and blue shifted Q-bands at 606-638 nm compared to corresponding freebase porphycenes. Notably, here also the positional effect of substituents could be clearly observed in these isomers with lowest energy bands of complexes of **1b** are red shifted compared to that of **1a**. Interestingly, both the metallo-derivatives of **1b** consist of split Q-bands, a trend also observed for complexes of octaethyl analogue **3**,<sup>6,13</sup> whereas, the split Soret bands observed in freebase porphycene **1a**, merged into one upon complexation with metal ions. The above trend clearly indicates, while **1a** behaves more like the octamethoxyporphycene **2**, its isomer **1b** resembles with the octaethyl analogue **3**. Unlike the porphycene **2**, which is non-fluorescent in nature ( $\phi_f < 10^{-4}$ ), the freebase porphycenes **1a** and **1b** are weakly emissive ( $\phi_f$  for **1a** and **1b**: 0.0007) with emission maxima at 655 and 676 nm, respectively (Fig. 1 and Table S1 in ESI<sup>†</sup>). Complexation with Zn(II) led to substantial enhancement in emission for both **Zn1a** and **Zn1b** ( $\phi_f$  for **Zn1a**, 0.17 and **Zn1b**, 0.16) with emission maxima at 645 and 654 nm, respectively. More strikingly, replacement of four

methoxy group of **Zn2** ( $\phi_f$  0.025),<sup>6</sup> with chloro groups (**Zn1a** and **Zn1b**) resulted in large enhancement of their fluorescence, indicating electron donating methoxy groups probably act as quencher of fluorescence through enhanced intramolecular charge transfer (ICT).<sup>2f</sup> This is again reflected in the relatively longer fluorescence lifetime observed for **Zn1a** ( $\tau_f$  2.9 ns) than **Zn1b** ( $\tau_f$  2.2 ns) (Fig. S31 in ESI†) and the chloromethoxy-porphycene complexes displaying much longer singlet lifetime compared to octamethoxy analogue **Zn2** ( $\tau_f$  0.6 ns).<sup>6</sup>

The crystal structures of **1a** and **1b** along with their axially pyridine (Py) ligated Zn(II)-complexes i.e. **Zn1a.Py** and **Zn1b.Py** were characterized by XRD techniques (Fig. 2). The molecular structures of **1a** and **1b** display planar configuration (maximum displacement of N from mean plane drawn through macrocyclic core: 0.053 and 0.032 Å for **1a** and **1b**, respectively). As per our anticipation the presence of relatively smaller chloro groups at 3,6- and 13,16- positions in **1b**, didn't exert any distortion on macrocyclic core owing to lesser nonbonding interaction, unlike that reported for the tetrabromoporphycene **4**.<sup>14</sup> Also, crystal packing structures of **1a** and **1b** (Fig. S24 in ESI†) display strong face to face  $\pi$ - $\pi$



**Fig. 2** Molecular structures of (a) **1a** (above front and below side view) (d) **1b** (above front and below side view), (b) **Zn1a.Py** front view, (c) **Zn1a.Py** side view, (e) **Zn1b.Py** front view and (f) **Zn1b.Py** side view, scaled in 35% probability level. Pyridine from all front views (for Zn(II) complexes), and chloro and methoxy groups from all side views are removed for clarity. Color code: C, grey; N, blue; O, red; Cl, yellow green; H, white; Zn, pink.

stacking interaction with inter-planar distance of 3.42 and 3.49 Å, and corresponding centroid-centroid distance of 3.95 and 4.13 Å, respectively. A closer look at the packing diagrams of both the porphycenes reveal when the methoxy substituents are at the inner  $\beta$ -positions (**1a**), the  $\pi$ - $\pi$  stacking interaction is enhanced owing to interaction between the alternate methoxy O of one macrocycle and the methoxy H of the neighbouring macrocycle in the stack, with chloro groups not involved in further interactions (Fig. S25 in ESI†). On the other hand, when the methoxy substituents are at the outer  $\beta$ -positions (**1b**), the  $\pi$ - $\pi$  stacking interaction is slightly reduced, as owing to its unique structure, alternate chloro groups of each porphycene could come in close contact with two methoxy Hs of porphycene molecule in the neighbouring stack, further each methoxy O while interacts with the methoxy H of the macrocycle in the same stack, in addition also interact with that of the macrocycle in another neighboring stack (Fig. S26 in ESI†). In analogy to other octasubstituted porphycenes, **1a** and **1b** retain square type core (N1-N2: 2.78 Å, N2-N3: 2.715 Å and N1-N2: 2.727 Å,

N2-N3: 2.761 Å for **1a** and **1b**, respectively). Surprisingly, the core of **1a** is comparatively more rectangular in nature than **1b** and in case of the latter unexpectedly the core has undergone slight expansion in N2-N3 distance, with concomitant contraction in N1-N2 distance. This could be explained by relatively stronger in-plane nonbonding repulsion of chloro groups at 3,6- and 13,16- positions in **1b**. This is further supported by comparatively upfield shift of imino protons in <sup>1</sup>H NMR resulting from relatively weak N-H...N H-bonding interaction for **1b**. Thus we can conclude that the distinct substitution effects on absorption and emission properties of **1a** and **1b** arise from the in plane non-bonding interaction at 3,6- and 13,16-positions and the resultant change in core size.

The **Zn1a.Py** and **Zn1b.Py** complexes display typical rectangular core (Fig. 2). The axial coordination with pyridine led to Zn ion residing above the plane of the macrocycle in both cases. Interestingly, the axial ligation of Zn with pyridine, led to elevation of Zn along with substantial deformation of core of the macrocycle in case of **Zn1a.Py** to result in a cone shape formation, but in contrast, for **Zn1b.Py** only elevation of Zn is observed but core of macrocycle remains almost planar and this is further reflected in the degree of displacement of  $\beta$ -C's from mean plane drawn through four imino nitrogens with the maximum displacement observed is 0.72 and 0.17 Å, respectively. Also, displacement of imino Ns from the mean plane drawn through macrocycle is 0.22 and 0.04 Å, respectively for **Zn1a.Py** and **Zn1b.Py** indicating a relatively more planar core for latter. Again a closer inspection of the packing diagram of both the complexes divulge in case of **Zn1b.Py**, there is weak  $\pi$ - $\pi$  stacking interaction between two porphycene moieties (inter-planar distance 3.49 Å and centroid to centroid distance 6.89 Å), whereas in case of **Zn1a.Py**, very interestingly the axially ligated pyridine moiety from a neighbouring porphycene unit slips into the two porphycene moieties involved in  $\pi$ - $\pi$  stacking interaction (Fig. S27-28 in ESI†). As a result the pyridine moiety has better stacking with one of the two porphycene units, while reducing the interaction between the latter. The combined effect possibly resulted in the large out of plane distortion in **Zn1a.Py** complex. These attributes clearly demonstrate further the positional effect of substituents, even in case of the metallo-porphycenes.

The NIR singlet oxygen luminescent spectra (emission maxima ~1278 nm) of all porphycenes in aerated toluene were measured in order to evaluate their singlet oxygen generation ability. Unlike **4**,<sup>14</sup> freebase porphycenes **1a** and **1b** could not able to produce singlet oxygen, indicating probably chloro groups can't effectively enhance triplet population, a key requirement for singlet oxygen generation. However, upon complexation we could observe effective singlet oxygen generation, with quantum yield ( $\phi_\Delta$ ) for **Zn1a** and **Zn1b**, 0.73 and 0.57, respectively and that for **Pd1a** and **Pd1b**, 0.86 and 0.83, respectively (Fig. S30 in ESI†). There is a substantial enhancement in singlet oxygen quantum yield by replacing four methoxy groups of analogous metal complexes of **2** ( $\phi_\Delta$  for **Zn2** and **Pd2** 0.12 and 0.73, respectively) with chloro groups. This clearly indicates the electron donating methoxy groups act as triplet state quencher through effective ICT character and possibly more efficiently at the outer  $\beta$ -positions, and the presence of electron withdrawing chloro groups, probably counter the ICT process, thereby enhancing the fluorescence, singlet state lifetime and also the singlet oxygen generation ability compared to octamethoxyporphycenes.<sup>6</sup>

The electrochemical properties of porphycene **1a**, **1b** and their Zn(II) complexes were characterized by cyclic

voltammetry (CV) and differential pulse voltammetry (DPV) in  $\text{CH}_2\text{Cl}_2$  (Fig. S32 in ESI† and Table 1) and that of the Pd(II) complexes couldn't be performed due to their poor solubility. These porphycenes and their Zn(II) complexes display typical two reversible and/or quasi reversible one electron reduction and two one electron oxidation potentials. Introduction of four chloro groups by replacing methoxy groups of **2** leads to more positively shifted oxidation and reduction potentials. The first reduction potential is 0.51 and 0.55 V more positive and similarly first oxidation potential is 0.37 and 0.38 V more positive, respectively for **1a** and **1b** compare to octamethoxy analogue **2**,<sup>6</sup> confirming the relatively more electron deficient nature of both the macrocycles. Also, the more positive change

**Table 1** Redox Potentials (in V vs SCE) for Porphycenes and Their Zn(II) Complexes

Porphycenes	Reduction	Oxidation	( $\Delta E$ )
<b>1a</b>	-0.81, -0.60	+1.15 <sup>a</sup> , +1.29 <sup>a</sup>	1.75
<b>1b</b>	-0.73, -0.56	+1.16 <sup>a</sup> , +1.39 <sup>a</sup>	1.72
<b>Zn1a</b> <sup>b</sup>	-1.20 <sup>b</sup> , -0.89	+0.99, +1.23	1.88
<b>Zn1b</b> <sup>b</sup>	-0.83	+0.96, +1.11 <sup>a</sup>	1.79
<b>2</b> <sup>c</sup>	-1.29, -1.11	+0.78, +1.15	1.89
<b>Zn2</b> <sup>c</sup>	-1.38, -1.13	+0.60, +0.75	1.73

<sup>a</sup> measured by DPV, <sup>b</sup> ~50  $\mu\text{L}$  THF was added to enhance solubility, <sup>c</sup> taken from ref 6.

in reduction potential compare to oxidation potential proves that LUMO is more stabilized compare to HOMO upon introduction of four chloro groups. Surprisingly, the positional effect of substituents on the redox potentials of these porphycenes is found to be minimal, in particular for the first oxidation and reduction potentials. Further, all Zn(II) complexes (**Zn1a** and **Zn1b**) show more positive reduction potential and oxidation potentials compared to analogous **Zn2**.<sup>6</sup> The experimental HOMO-LUMO gap ( $\Delta E$  measured from CV) for porphycene **1a** and **1b** found to be 1.75 and 1.72 V, respectively, which is 0.14 and 0.17 V lower compare to **2**.<sup>6</sup> The marginal difference in  $\Delta E$  between the two isomers is again reflected in the computationally obtained data by single point calculation of crystal structures of **1a** and **1b** by using B3LYP (6-31+G) method (Fig. S37 in ESI†).<sup>15</sup> This may be attributed to cancellation of the electronic effect of the substituents owing to their symmetrically opposite disposition at the macrocycle periphery (dipole moment obtained from DFT study is zero for both **1a** and **1b**).

In conclusion, we have synthesized the first chloro substituted porphycenes, namely  $\beta$ -tetrachlorotetramethoxy-porphycenes as two positional isomers, regiospecifically. The oxidative coupling of protected pyrrole aldehyde enables us to synthesize bipyrrrole dialdehydes in three steps from pyrrole aldehyde and this strategy helps avoid unstable  $\alpha$ -free bipyrrrole intermediate. This protocol can also be used for regiospecific synthesis of porphycene isomers. Further, the positional effects of substituents in porphycene is investigated for the first time and owing to the presence of two  $\alpha$ - $\alpha'$  fused bipyrrrolic units, the substituents exert significant positional effect on structure and photophysical properties of these porphycenes, including their metallo-derivatives. In addition, all the metalloporphycenes effectively generate singlet oxygen and therefore may find applicability as efficient photosensitizers for PDT along with photo inactivation of bacteria and viruses, and for photo-oxidation.

This work is supported by DST, India (SR/S1/IC-56/2012 to P.K.P). A.R. thanks CSIR, India for senior research fellowship and DRDO, India for financial assistance. The authors also thank Mr. Navendu Mondol and Mr. B. Sathish Kumar, School

of Chemistry, University of Hyderabad for the fluorescence lifetime and DFT studies, respectively.

## Notes and references

<sup>a</sup> School of Chemistry and Advance Centre of Research in High Energy Materials (ACRHEM), University of Hyderabad, Hyderabad-500046, India.

† Electronic Supplementary Information (ESI) available: Detailed synthetic procedure, characterization, photophysical data and crystal data (CIF). CCDC No. 1062094–1062100. See DOI: 10.1039/c000000x/

- (a) E. Vogel, M. Kocher, H. Schmickler and J. Lex, *Angew. Chem. Int. Ed. Engl.*, 1986, **25**, 257; (b) D. Sánchez-García and J. L. Sessler, *Chem. Soc. Rev.*, 2008, **37**, 215; (c) J. C. Stockert, M. Cañete, A. Juarranz, A. Villanueva, R. W. Horobin, J. I. Borrell, J. Teixidó and S. Nonell, *Curr. Med. Chem.*, 2007, **14**, 997.
- (a) T. Matsuo, H. Dejima, S. Hirota, D. Murata, H. Sato, T. Ikegami, H. Hori, Y. Hisaeda and T. Hayashi, *J. Am. Chem. Soc.*, 2004, **126**, 16007; (b) T. Hayashi, K. Okazaki, N. Urakawa, H. Shimakoshi, J. L. Sessler, E. Vogel and Y. Hisaeda, *Organometallics*, 2001, **20**, 3074; (c) W. Brenner, J. Malig, R. D. Costa, D. M. Guldi and N. Jux, *Adv. Mater.*, 2013, **25**, 2314; (d) J. Arnbjerg, A. Jiménez-Banzo, M. J. Paterson, S. Nonell, J. I. Borrell, O. Christiansen and P. R. Ogliby, *J. Am. Chem. Soc.*, 2007, **129**, 5188; (e) T. Sarma, P. K. Panda, P. T. Anusha and S. V. Rao, *Org. Lett.*, 2011, **13**, 188; (f) A. Rana, S. Lee, D. Kim and P. K. Panda, *Chem. Commun.*, 2015, **51**, 7705; (g) S. Feihl, R. D. Costa, W. Brenner, J. T. Margraf, R. Casillas, O. Langmar, A. Browa, T. E. Shubina, T. Clark, N. Jux and D. M. Guldi, *Chem. Commun.*, 2014, **50**, 11339; (h) H. Saeki, O. Kurimoto, H. Nakaoka, M. Misaki, D. Kuzuhara, H. Yamada, K. Ishida and Y. Ueda, *J. Mater. Chem. C*, 2014, **2**, 5357.
- (a) P. Ciąćka, A. Listkowski, M. Kijak, S. Nonell, D. Kuzuhara, H. Yamada, C. Radzewicz and J. Waluk, *J. Phys. Chem. B*, 2015, **119**, 2292; (b) T. Kumagai, F. Hanke, S. Gawinkowski, J. Sharp, K. Kotsis, J. Waluk, M. Persson and L. Grill, *Nature Chem.*, 2014, **6**, 41.
- K. Oohora, A. Ogawa, T. Fukuda, A. Onoda, J.-y. Hasegawa and T. Hayashi, *Angew. Chem. Int. Ed.*, 2015, **54**, 6227.
- (a) K. S. Anju, S. Ramakrishnan, A. P. Thomas, E. Suresh and A. Srinivasan, *Org. Lett.*, 2008, **10**, 5545; (b) E. Ganapathi, T. Chatterjee and M. Ravikanth, *Eur. J. Org. Chem.*, 2014, 6701.
- A. Rana, and P. K. Panda, *Org. Lett.*, 2014, **16**, 78.
- A. Rana and P. K. Panda, *Tetrahedron Lett.*, 2011, **52**, 2697.
- C. Mazat and L. H. Gade, *Chem. -Eur. J.*, 2002, **8**, 4308.
- L. Jiao, E. Hao, G. H. Vincente and K. M. Smith, *J. Org. Chem.*, 2007, **72**, 8119.
- J. B. Paine III and D. Dolphin, *J. Org. Chem.*, 1988, **53**, 2787.
- H. Falk and H. Flödl, *Monatsh. Chem.*, 1988, **119**, 247.
- M. Grzybowski, K. Skonieczny, H. Butenschön and D. T. Gryko, *Angew. Chem. Int. Ed.*, 2013, **52**, 9900.
- E. Vogel, P. Koch, X.-L. Hou, J. Lex, M. Lausmann, M. Kisters, M. A. Aukaaloo, P. Richard and R. Guillard, *Angew. Chem. Int. Ed. Engl.*, 1993, **32**, 1600.
- H. Shimakoshi, T. Baba, Y. Iseki, I. Aritome, A. Endo, C. Adachi and Y. Hisaeda, *Chem. Commun.*, 2008, 2882.
- Gaussian 09, (Revision C. 01), M. J. Frisch, et al. Gaussian, Inc. Wallingford CT, 2010. For full reference, see ESI†.